

Magnetically-Tuned Kondo Effect in a Molecular Double Quantum Dot: Role of the Anisotropic Exchange

Peter Zalom,^{†,§} Joeri de Bruijckere,[‡] Rocco Gaudenzi,^{‡,¶} Herre S. J. van der Zant,[‡] Tomáš Novotný,[†] and Richard Korytár^{*,†}

[†]*Department of Condensed Matter Physics, Faculty of Mathematics and Physics, Charles University, Ke Karlovu 5, 121 16 Praha 2, Czech Republic*

[‡]*Kavli Institute of Nanoscience, Delft University of Technology, 2628 CJ Delft, The Netherlands*

[¶]*Max Planck Institute for the History of Science, Boltzmannstrasse 22, 14195 Berlin, Germany*

[§]*Institute of Physics, The Czech Academy of Sciences, Na Slovance 2, CZ-18221 Praha 8, Czech Republic*

E-mail: korytar@karlov.mff.cuni.cz

Abstract

We investigate theoretically and experimentally the singlet-triplet Kondo effect induced by a magnetic field in a molecular junction. Temperature dependent conductance, $G(T)$, is calculated by the numerical renormalization group, showing a strong imprint of the relevant low energy scales, such as the Kondo temperature, exchange and singlet-triplet splitting. We demonstrate the stability of the singlet-triplet Kondo effect against weak spin anisotropy, modeled by an anisotropic exchange. Moderate spin anisotropy manifests itself by lowering the Kondo plateaus, causing the $G(T)$ to deviate from a standard temperature dependence, expected for a spin-half Kondo effect. We propose this scenario as an explanation for anomalous $G(T)$, measured in an organic diradical molecule coupled to gold contacts. We uncover certain new aspects of the singlet-triplet Kondo effect, such as coexistence of spin-polarization on the molecule with Kondo screening and non-perturbative parametric dependence of an effective magnetic field induced by the leads.

Introduction

Electronic transport through single molecules with open shells allows the investigation of many fascinating phenomena which are rooted in the physics of the Coulomb blockade. A prominent example is the observation of an underscreened Kondo effect on a single entity, the Au+C₆₀ junction.¹ Other examples are the SU(4) Kondo effect^{2,3} or a quantum phase transition driven by the gate voltage.⁴ The reproducible and sharply defined chemical structure of molecules could unveil new aspects of the Coulomb blockade physics, such as many-body quantum interference.⁵

Molecules with two open-shell orbitals share certain features with the so-called *double quantum dots* (DQDs) and can be theoretically modeled by an Anderson or Kondo model with two “impurity” spins. These models exhibit a rich phenomenology, *e.g.*, Refs. 6–11. Here we focus on a specific case when the two spins couple antiferromagnetically and are subjected to an external magnetic field. The low-energy spectrum of such an isolated molecule can be ap-

proximately captured by the Hamiltonian

$$\hat{H}_{\mathcal{M}} = I\mathbf{S}_1 \cdot \mathbf{S}_2 + g\mu_B\mathbf{B} \cdot (\mathbf{S}_1 + \mathbf{S}_2), \quad (1)$$

expressed through the spin operators \mathbf{S}_1 and \mathbf{S}_2 . The first term in Eq. (1) describes the anti-ferromagnetic interaction ($I > 0$) and the second term is the Zeeman term, corresponding to a homogeneous magnetic field \mathbf{B} . We show the magnetic field dependence of the molecular spectrum in Scheme 1c, adopting the units $g\mu_B = 1$. The ground-state has an accidental two-fold degeneracy if $|\mathbf{B}| = I$. The resulting effective two-level system, when coupled to leads, exhibits the Kondo effect, as predicted in Refs. 12,13.

Recently, the DQD has gained renewed attention, because it can host topologically-protected Weyl points. The Weyl points are particular ground-state degeneracies which have incarnations in diverse physical contexts, such as molecular conical intersections,¹⁴ semi-metal band-structures,¹⁵ or quantum field theory.¹⁶ In the DQD model, the Weyl points emerge when spin-orbit effects are considered. Spin-orbit interaction effectively leads to the addition of spin anisotropies in Eq. (1), namely, anisotropic exchange interaction and anisotropic (and dot-dependent) g -tensor.^{17,18} As long as the anisotropies are weak, a ground-state degeneracy can be found for at least two magnetic fields $\pm\mathbf{B}_0$ related by time-reversal. These Weyl points were recently reported in InAs DQD¹⁹ by means of a transport spectroscopy. When the magnetic field is tuned to the degeneracy, Scherübl et al. observe a Kondo resonance.

Motivated by the significance of such magnetic-field induced level crossings, we revisit the transport properties of the DQD near a degeneracy point. We present a combined experimental and theoretical effort. In the experimental part of this work, we show conductance measurements of a molecular junction: a 2,4,6-hexakis-(pentachlorophenyl)mesitylene diradical bound to gold contacts. This molecule (see Scheme 1a) represents a prototypical molecular DQD, where the two spins sit on the radical sites. When the magnetic field is tuned to a

ground-state degeneracy, a Kondo-like zero-bias anomaly (ZBA) is observed. Intriguingly, the temperature dependence of the ZBA does not follow a standard, universal behavior of a Kondo impurity.

Thus motivated, we perform a comprehensive theoretical analysis of the conductance of the DQD model in the vicinity of the magnetic-field induced ground-state degeneracy. Our results include the effects of weak spin anisotropy. We calculate the conductance by the numerical renormalization group (NRG) technique. Our results complement earlier perturbative studies of the anisotropy effects in the DQD,^{18,20} because NRG allows us to address quantum spin-fluctuations, which eventually lead to the singlet-triplet Kondo effect. We offer a plausible and robust explanation of the anomalous temperature dependence observed in our experiment. Moreover, we reveal and analyze certain new aspects of the DQD, such as coexistence of spin polarization and Kondo screening at the degeneracy point and effective magnetic field induced by the leads.

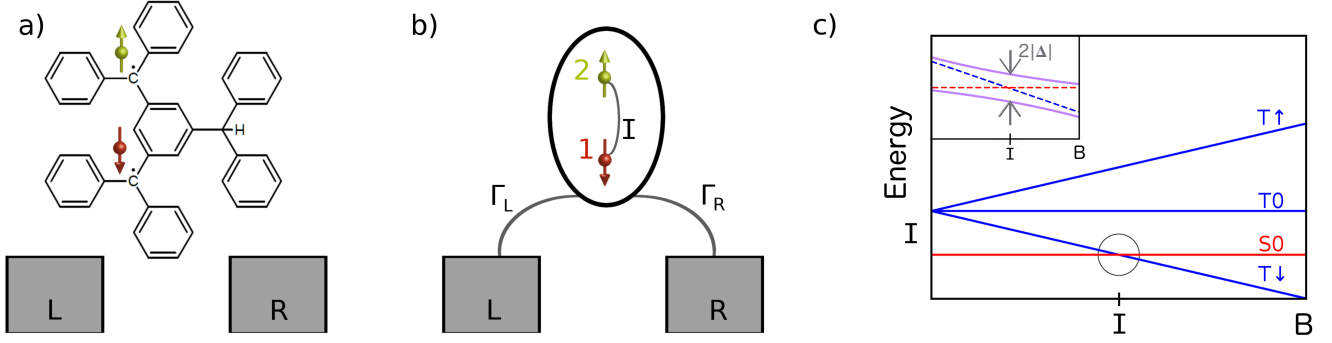
Methods

Theoretical Methods

Double Quantum Dot in a Magnetic Field

We introduce a model of a molecule coupled to two leads in which the singlet-triplet degeneracy can be achieved by an external magnetic field. We shall assume that the low-energy excitations are spin-excitations due to exchange-coupled spins residing in two orbitals (two “quantum dots”). Such a model can apply to organometallic complexes with two open-shell transition-metal centers, organic diradicals (see an example given in Scheme 1) and other open-shell molecules with even number of electrons (for instance, Ref.⁴).

Coupling the molecule to a pair of leads induces Kondo correlations, which generally involve two screening channels.^{5,13} The two screening channels can be characterized by two characteristic temperature scales (Kondo temperatures), T_1 and T_2 .¹³ In a general molecular-



Scheme 1: (a) Illustration of a diradical molecule [2,4,6-hexakis-(pentachlorophenyl)mesitylene] coupled to a pair of leads. (b) Schematic representation of the Hamiltonian: dot 1 couples to the leads, each lead introduces single-particle level broadening Γ_L , Γ_R . The dot 2 couples to dot 1 with an anti-ferromagnetic exchange. (c) Magnetic field dependence of the four lowest energy levels (eqs 3) of the double quantum dot. The accidental singlet-triplet degeneracy occurs when $B = I$. Inset: zoom of the crossing. When Dzyaloshinskii-Moryia interaction, Eq. (4), is considered, the original crossing (dashed lines) turns into an avoided crossing (purple lines) with the splitting $2|\Delta|$.

electronic setup, the coupling of the first and second dots to the leads is highly asymmetric, implying an exponential separation of T_1 and T_2 . Unless $T_1 \approx T_2$, the stronger coupled channel wins and the low-temperature behavior is equivalent to a fully-screened Kondo impurity. Thus, in a major portion of the parameter space the physics is of a single-channel type. We shall consider in this work single-channel effects only, and for this reason we can make simplifying assumptions on the details of the dot-lead couplings. Specifically, we will consider that only the first dot couples to the two leads, while the coupling of the second dot to the leads vanishes. We may thus disregard charge-fluctuations on the second dot and consider only its spin degree of freedom, represented by operator \mathbf{S}_2 .

The Hamiltonian of the DQD can be written as $H_{\text{DQD}} = H_1 + H_{\text{ex}} + H_Z$, where the individual terms read

$$H_1 = \sum_{\sigma} \varepsilon_d d_{\sigma}^{\dagger} d_{\sigma} + U n_{d,\uparrow} n_{d,\downarrow} \quad (2a)$$

$$H_{\text{ex}} = I \mathbf{S}_1 \cdot \mathbf{S}_2 \quad (2b)$$

$$H_Z = B \left(\hat{S}_{z,1} + \hat{S}_{z,2} \right). \quad (2c)$$

The term H_1 represents the first dot as an Anderson impurity. The operator d_{σ}^{\dagger} creates an electron of spin $\sigma \in \uparrow, \downarrow$, $n_{d,\sigma} = d_{\sigma}^{\dagger} d_{\sigma}$ is the number operator, ε_d is the onsite energy and U is the

charging energy. The term H_{ex} represents the antiferromagnetic exchange interaction ($I > 0$) between both dots. The operator \mathbf{S}_i is the spin operator of the respective dots. The operator \mathbf{S}_1 can be expressed in terms of Pauli matrices $(\sigma_x, \sigma_y, \sigma_z) = \boldsymbol{\sigma}$ as $\mathbf{S}_1 = \frac{1}{2} \sum_{\sigma''\sigma'} d_{\sigma'}^{\dagger} \boldsymbol{\sigma}_{\sigma'\sigma''} d_{\sigma''}$. Finally, the term H_Z represents the homogeneous magnetic field in the z -direction; the field strength B is represented in units of energy (*i.e.* $g\mu_B = 1$).

We investigate the properties of the DQD in the Coulomb blockade regime, *i.e.* when the occupancy of the first dot is approximately one. Hence, the following hierarchy of energy scales is assumed: $U, |\varepsilon_d| \gg |B|, I$ and $\varepsilon_d < 0 < U$. Consequently, the lowest-lying eigenstates of H_{DQD} are triplet and singlet and their energies

read

$$|T\uparrow\rangle = |\uparrow\uparrow\rangle, \quad E_{T\uparrow} = \varepsilon_d + B + \frac{I}{4} \quad (3a)$$

$$|T0\rangle = \frac{1}{\sqrt{2}} (|\uparrow\downarrow\rangle + |\downarrow\uparrow\rangle), \quad E_{T0} = \varepsilon_d + \frac{I}{4} \quad (3b)$$

$$|T\downarrow\rangle = |\downarrow\downarrow\rangle, \quad E_{T\downarrow} = \varepsilon_d - B + \frac{I}{4} \quad (3c)$$

$$|S0\rangle = \frac{1}{\sqrt{2}} (|\uparrow\downarrow\rangle - |\downarrow\uparrow\rangle), \quad E_{S0} = \varepsilon_d - \frac{3I}{4} \quad (3d)$$

where in the symbol $|\uparrow\downarrow\rangle$ the first (second) arrow represents the spin projection of the first (second) dot, respectively. The spectrum of H_{DQD} is shown in Scheme 1c, where we can recognize the ground-state degeneracy point at $B = I$.

Anisotropic Exchange

The Hamiltonian H_{DQD} introduced here enjoys rotational invariance in the spin space. This is an approximation, because the spin is not a good quantum number due to spin-orbit interaction (SOI). We shall assume that the latter is associated with the smallest energy scale (compared to U and I), which holds true for, e.g., organic molecules. The presence of weak SOI can be accounted for by anisotropies in the exchange (H_{ex}) and Zeeman (H_{Z}) terms.¹⁷ Since we consider effects related to the singlet-triplet crossing, the main effect of the anisotropies will be to split the degeneracy of the $|S0\rangle$ and $|T\downarrow\rangle$. As a function of B , the crossing becomes avoided, as shown in Scheme 1c.

Without loss of generality, we can consider a specific form of the anisotropy, the Dzyaloshinskii-Moriya interaction

$$H_A = -2\sqrt{2}\Delta \left(\hat{S}_1^x \hat{S}_2^z - \hat{S}_1^z \hat{S}_2^x \right), \quad (4)$$

where $2|\Delta|$ yields the singlet-triplet gap at $B = I$. The above interaction exhibits a special direction, the y -axis, which is commonly refer-

enced to as a Dzyaloshinskii-Moriya vector. We note that the level crossing induced by H_A can be restored by rotating the magnetic field to the y -axis.¹⁸

Coupling to the Leads and Conductance

The complete Hamiltonian of the molecule coupled to (left and right) leads consists of three terms $H = H_{\text{DQD}} + H_1 + H_t$, where the subscript labels denote the double quantum dot, leads and tunneling. The lead Hamiltonian has a standard form

$$H_1 = \sum_{x,k\sigma} \varepsilon_{x,k} c_{x,k\sigma}^\dagger c_{x,k\sigma}, \quad (5)$$

where $c_{x,k\sigma}^\dagger$ is a canonical creation operator and $\varepsilon_{x,k}$ are single-particle energies. The indices denote spin σ , lead $x = \text{L,R}$ (for left and right) and the remaining quantum numbers (e.g. bands and wave-numbers) are encapsulated in k . The coupling between the leads and the DQD is given by the tunneling Hamiltonian H_t of the form

$$H_t = \sum_{x,k\sigma} V_{x,k} c_{x,k\sigma}^\dagger d_\sigma + \text{h. c.}, \quad (6)$$

where $V_{x,k}$ is the hybridization matrix element and h.c. stands for Hermitian conjugate. Each lead gives rise to a single-particle hybridization function defined by $\Gamma_x(\varepsilon) = \pi \sum_{\mathbf{k}} |V_{x,\mathbf{k}}|^2 \delta(\varepsilon - \varepsilon_{x,\mathbf{k}})$. We employed hybridization functions that are constant within a bandwidth $2D$, *i.e.*: $\Gamma_x(\varepsilon) = \Gamma_x \theta(D - |\varepsilon|)$.

Near the degeneracy point, the Hamiltonian H [Eqs.(2, 4-6)] describes a single-channel Kondo problem. As stated earlier, a non-vanishing coupling of the dot 2 to the leads would imply a two-channel problem, however, the latter is not commonly expressed in molecular junctions, as the dominant screening channel takes over, so the problem is effectively single channel. A further consequence of having both dots coupled to conduction electrons is that an effective exchange coupling $I_{\text{RKKY}} \mathbf{S}_1 \cdot \mathbf{S}_2$ of the Rudermann-Kittel-Kasuya-type emerges.⁸ Hence, the effect of the coupling of dot 2 to leads can be seen as a renormaliza-

tion of the exchange I .

For the (linear) conductance the following relationship holds

$$G(T) = \frac{2e^2}{h} \frac{4\Gamma_L\Gamma_R}{(\Gamma_L + \Gamma_R)^2} \times \int_{-\infty}^{\infty} d\omega \pi\Gamma A_1(\omega) [-n'_F(\omega)] \quad (7)$$

where $\Gamma \equiv \Gamma_L + \Gamma_R$, the derivative of the Fermi-Dirac distribution is denoted by n'_F , and $A_1(\omega)$ is the spectral function of the first dot. The only effect of the asymmetry of the couplings to both leads is to modify the prefactor of the integral in Eq. (7). This motivates us to introduce the conductance unit

$$G_0 \equiv \frac{2e^2}{h} \frac{4\Gamma_L\Gamma_R}{(\Gamma_L + \Gamma_R)^2}. \quad (8)$$

Estimates of the Energetic Scales in the Molecular Problem

The model that we introduced is based on considerable simplifications of the electronic structure of the molecule coupled to leads. The simplifications can be justified by the fact that the emergent low-temperature Kondo physics is always governed by only few parameters (*e.g.* T_K , G_0 , I , Δ). However, these parameters do not directly relate to the energy scales of the molecule in isolation due to interactions between the molecule and contacts. We give our estimates in what follows.

The exchange coupling I characteristic of isolated organic diradicals can be (typically) 40 meV $> I > 0.4$ meV.²¹ As we remarked, the hybridization of both “dots” with the leads can slightly renormalize I . The parameter Δ causes spin anisotropy, and can be estimated by zero-field splittings. For the diradicals, the values $\approx 50\mu\text{eV}$ have been reported, for instance in Ref.²² The value of U can be obtained from charging energy in the gas-phase, however, the latter is considerably screened by the lead electrons. We estimate the value of the order of $U \approx 100$ meV. The energy scale $|\varepsilon_d|$ of an Anderson impurity is, in principle, the approximate ionization energy of the molecule coupled to the leads. It is unfortunately not possible

to estimate ε_d from gas-phase ionization levels because the alignment of the ionization level with the Fermi energy of the metal contacts is affected by partial charge transfer. Moreover, some molecular transport experiments operate with a gate voltage, allowing the effective tuning of the value of ε_d . The single-particle energetic broadening Γ is on the order of 5 meV²³ and it is sensitive to the binding geometry.

Numerical Renormalization Group Calculations

For the numerical analysis of the present double-dot model, we have utilized the open-source code NRG LJUBLJANA.^{24,25} The spectral functions have been obtained by the full density matrix algorithm based on the complete Fock-space concept.^{24,26} The interleaved method has been used to smoothen the resulting spectral functions^{24,26} while the logarithmic discretization parameter has been set to $\Lambda = 2$. All results are obtained for $\varepsilon_d = -U/2$.

Experimental Methods

The molecule used here is a 2,4,6-hexakis-(pentachlorophenyl)mesitylene diradical²⁷ depicted in Scheme 1a. The single-molecule device used for the transport measurements is similar to the one used in Ref. 23. By electromigration²⁸ and self-breaking²⁹ of a gold nanowire, a nanometer-sized gap is formed, in which molecules can be trapped to realize a single-molecule junction. After electromigration, a dilute solution of the molecules of interest is drop-cast on a chip with 24 electromigrated gold nanowires. After pumping away the solution and cooling down the system in a dilution refrigerator ($T \approx 40$ mK), we typically find transport signatures of single molecules in 2 to 5 junctions per chip. We measure the DC current I through the single-molecule devices as a function of the applied bias voltage V over the junction, the voltage applied to a capacitively coupled gate electrode V_g , the temperature T (20 mK $< T < 4.2$ K), and the magnetic field B .

Results and discussion

Temperature Dependence of the Conductance

For the sake of reference, we start by presenting the conductance of the SIAM. We note that when $B = I = 0$ in Eq. (2), the transport properties of the DQD are equivalent to the SIAM, because the second dot is decoupled. We choose the parameters $U = D$ (used throughout the whole paper) and $\Gamma = 0.05D$, which correspond to the Coulomb blockade regime. In Figure 1 the black curve represents the temperature-dependent conductance $G(T)$, which exhibits a familiar low-temperature plateau due to the Kondo effect with $T_K(\text{SIAM}) \approx 5 \cdot 10^{-5}D$ (estimated from $G(T_K) = G_0/2$). For intermediate temperatures the conductance is suppressed, until T reaches the temperature scale of the charge excitations $U/2$.

In the next step we couple the second dot: we choose $I = 10^{-3}D$ so that the lowest-lying states of the isolated DQD are $|S0\rangle$ and $|T\sigma'\rangle$, *i.e.* singlet and triplet states. Figure 1 shows the conductances for different values of the Zeeman energy B , chosen so that $B \sim I$. The high- T part of $G(T)$ is almost identical to SIAM, the differences show up at low temperatures, when $T \lesssim I$. For $B = 0.8I$ the ground state of the isolated DQD is $|S0\rangle$ and the lowest-lying excited state is $|T\downarrow\rangle$, separated by an energy gap $I - B > T_K(\text{SIAM})$. The Kondo plateau is thus suppressed for this value of B . The bump for $10^{-5} < T < 10^{-2}$ corresponds to energy scales of spin excitations. Indeed, within the independent-particle picture, the elevated conductance can be traced to two effects: the thermal population of the $|T\sigma'\rangle$ states and the thermal broadening of the Fermi distribution of conduction electrons (see, e.g., Ref. 30).

When increasing the value of B toward I , the singlet-triplet degeneracy point is approached and the low-temperature plateau emerges. When $B = 0.9I$, the spectral function shows a split-peak (inset of Figure 1), in qualitative agreement with Ref. 31. For $B = 0.915I$, $G(0)$ reaches the unitary limit (red curve in Figure 1). When the temperature dependences are

compared to the SIAM, we observe two significant differences: First, the Kondo temperature of the DQD is suppressed by a factor $\approx 10^{-1}$. Second, the spin excitations give rise to the bump at $T \approx I$.

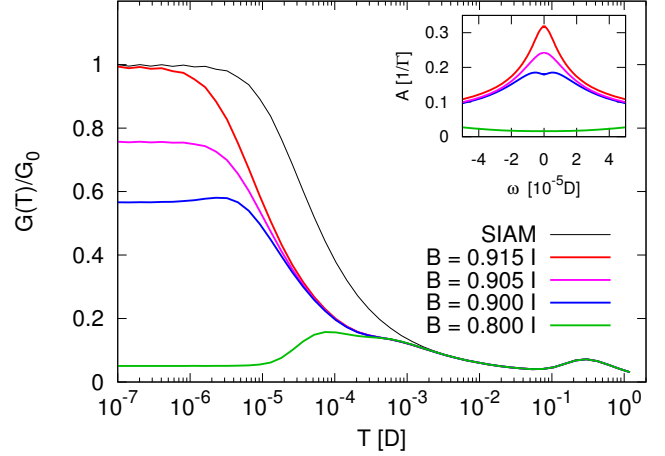


Figure 1: NRG results on the double-dot model: temperature dependence of the conductance in units of G_0 (eq 8) for the exchange coupling $I = 10^{-3}D$, broadening $\Gamma = 0.05D$ and various values of B . For comparison, we also show the conductance of the single-impurity Anderson model ($I = B = 0$). The inset shows the corresponding zero-temperature spectral functions.

Renormalization of the Resonant Magnetic Field

The above observations are consistent with the Kondo effect, which is induced by magnetically tuning the DQD to a degeneracy point, as predicted by Pustilnik et al. in Ref. 12. The unitary conductance is, however, not observed at $B = I$, as we demonstrate in Figure 2, where we show the zero-temperature conductance as a function of B . We denote the location of the maxima of the conductance as B^* and observe that the latter are consistently shifted toward lower values, below the “bare” degeneracy condition $B = I$. The difference $I - B^*$ can be understood as an effective magnetic field generated by the leads. This effect was described as a shift of the degeneracy point in

Refs. 12,13,18,31,32 but it was not analyzed in more detail.³³

To inspect the effective magnetic field more closely, we fixed I and changed the hybridization strength Γ . The values of $G(0)$ plotted against the external magnetic field B are presented in Figure 3. The width of the resonant peak tends sharply to zero with decreasing Γ . This observation can be rationalized by the concomitant (exponential) decrease of T_K , causing the Kondo resonance to be less robust as the magnetic field departs from the degeneracy point. The resonance field B^* tends to the bare value I as Γ decreases, as shown in the inset of Figure 3. The effective field can be fit by a power-law $I - B^* \propto \Gamma^\alpha$ with $\alpha = 2.22 \pm 0.08$.

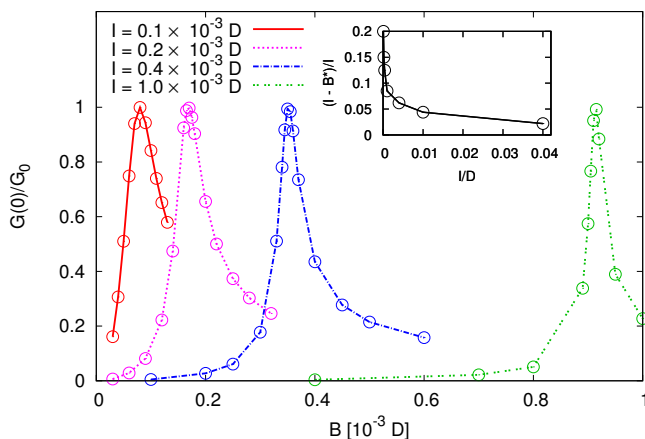


Figure 2: Theoretical zero-temperature conductance $G(0)$ as a function of the external magnetic field B for various values of I ($\Gamma = 0.05D$ is fixed). The locations of the maxima define the resonant field B^* . The difference $I - B^*$ can be interpreted as an effective field generated by the leads. Lines are only for visual guidance. The inset shows the dependence of the normalized effective magnetic field $(I - B^*)/I$ on I .

The presence of an effective magnetic field acting on the DQD is rooted in the fact that the two states $|S_0\rangle$ and $|T_\downarrow\rangle$ have a different orbital structure. Thus, the leads renormalize the energies $E_{S_0}, E_{T_\downarrow}$ in a different way. This can be contrasted with the SIAM, where the spin-up and spin-down states are related by an inversion of the spin quantization axis. The latter

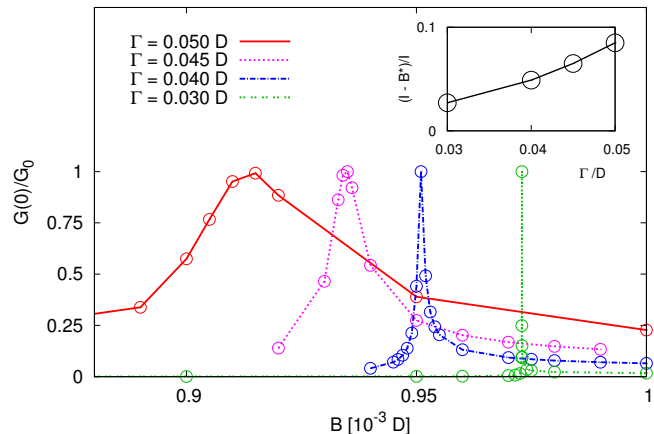


Figure 3: Theoretical zero-temperature conductance $G(0)$ as a function of the external magnetic field B for various values of Γ ($I = 10^{-3}D$ is fixed). Lines are only for visual guidance. The inset shows the dependence of the normalized effective magnetic field $(I - B^*)/I$ on Γ .

is a symmetry operation of the leads. Consequently, no effective magnetic field can be generated in the SIAM. The intriguing parametric dependence of B^* points to a non-perturbative nature of the effective magnetic field.

Spin-Polarization of the Kondo-Screened Dots

We explore another peculiar consequence of the broken spin-inversion symmetry. In Figure 4 we plot the z -component of the spins of the two dots as a function of I . We emphasize that the magnetic field is always tuned to the resonance B^* , *i.e.*, the conductance is unitary. Surprisingly, despite the Kondo screening, the two dots exhibit fractional spin polarization, which depends continuously on I .

We can understand the expectation values of spin in two simple limits: $I \ll T_K(\text{SIAM})$ and $I \gg T_K(\text{SIAM})$. For $I = 0$ it is seen that $S_z(1) = 0$, as expected for the SIAM with the first dot fully screened. The second dot is decoupled and its spin aligns along the field. When $0 < I \ll T_K(\text{SIAM})$, the second dot couples antiferromagnetically to the local Fermi-liquid excitations of the first Kondo-screened dot. It is known that when $B = 0$, second-

stage Kondo screening develops, with a characteristic temperature $T_K^{(2)}$, below which the conductance is suppressed.⁹ In our case, the external magnetic field is always tuned to achieve $G(0) = 1 \cdot G_0$, so that the two-stage screening is avoided.

In the opposite limit of large I we can see that both spins approach $-1/4$. As long as charge-fluctuations can be neglected, the latter result can be rationalized as follows: in the large- I limit, the DQD can be approximately described as a two-level system (TLS), the levels being $|S0\rangle$ and $|T\downarrow\rangle$. The expectation values of spin of either dot ($i = 1, 2$) in these states are $\langle S0 | \hat{S}_z(i) | S0 \rangle = 0$ and $\langle T\downarrow | \hat{S}_z(i) | T\downarrow \rangle = -1/2$. The interaction of the TLS with the leads can be described by an anisotropic Kondo Hamiltonian, as elaborated in Ref. 13. When $B = B^*$ (and $T = 0$) there is the Kondo effect, so that the two states have equal weights in the reduced density matrix. It follows that the expectation value of spin on both dots must be the equal average of 0 and $-1/2$, *i.e.*, $-1/4$.

In Figure 4 we see that even when $I \gg T_K \approx 10^{-4}D$, the deviation of $S_z(i)$ from $-1/4$ amounts to 10% or more. While the observation of Kondo plateaus (see Figure 1) can be consistently accounted for by the anisotropic Kondo Hamiltonian, other observables, such as the spin, are not consistent with this model. The spin polarization hints at sizable admixture of states $|T0\rangle$ and $|T\uparrow\rangle$ in the many-body ground-state. An effective low-energy model of the DQD should also include the latter states in order to account for the spin polarization.

Effects of Anisotropic Exchange

We have shown that despite the presence of the effective magnetic field generated by the leads, the Kondo plateaus can be reached by tuning the external magnetic field slightly away from the bare resonance condition $B = I$. We show below that this does not hold true, if the anisotropic exchange (AX) of the form in Eq. (4) is introduced.

Figure 5 shows the dependence of the conductance at zero temperature for a varying magnetic field. The effect of AX is to lower the peak

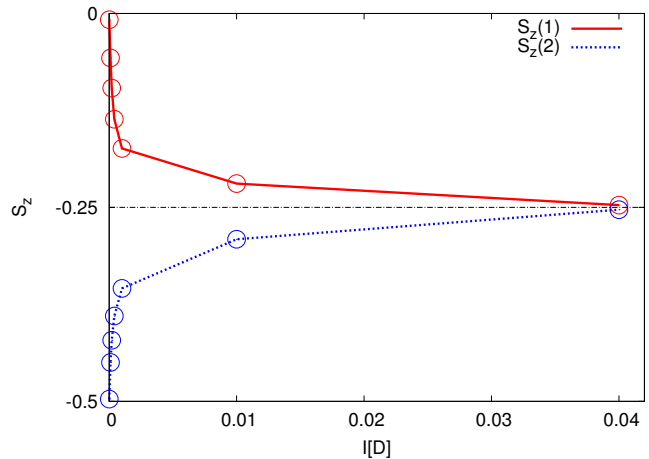


Figure 4: z -component of the spin of the primary (label 1, red full curve) and secondary (label 2, blue dashed curve) dot as a function of I . Lines are only for visual guidance.

value of the conductance and shift its location. The lowering of the peak value is caused by lowering of the Kondo plateaus in the temperature dependence, as shown in Figure 6.

This behavior can be understood in a simpler physical picture of the TLS on the subspace spanned by the two lowest-energy states $|S0\rangle$ and $|T\downarrow\rangle$. We shall denote the two states by $|\uparrow\rangle$ and $|\downarrow\rangle$. The matrix elements of H_A in the TLS are identical with the matrix elements of $\Delta\sigma_x$, where σ_x is the Pauli matrix. On the other hand, the energy gap between the two states can be represented by $\frac{1}{2}\tilde{B}_z\sigma_z$. The \tilde{B}_z incorporates the bare splitting $I - B$, as well as the effective field. In the TLS picture it is easy to see that the AX destroys the Kondo effect and that the latter can not be restored by tuning B , because $\Delta\sigma_x$ causes an avoided level crossing.

We underline two important observations made from Figure 6: First, the conductance plateaus are not destroyed by small AX ($\Delta = 10^{-6}D < T_K$). Second, the Kondo peak diminishes and splits with increasing Δ . This behavior is reminiscent of the behavior of a standard spin-half Kondo impurity in a magnetic field. There, a small Zeeman splitting (much smaller than the Kondo temperature) does not destroy the conductance plateau (it is a “marginal” term) and leads to the peak splitting.^{34–36} Con-

cluding, we have shown that the robustness of the Kondo plateaus is consistent with the interpretation of the AX as a pseudo-magnetic field acting on the TLS.

While in our calculation, we use only a specific form of the AX with the Dzyaloshinskii-Moriya vector (DMV) aligned with the y -axis, it can be seen that a general DMV translates into the TLS as a pseudo-magnetic field, represented by a linear combination of σ_x and σ_y matrices. Only when the DMV is parallel with the z -axis (the direction of the external magnetic field), the matrix elements of the AX in the TLS vanish. The crossing is preserved in this special case, as pointed out also in Ref. 18.

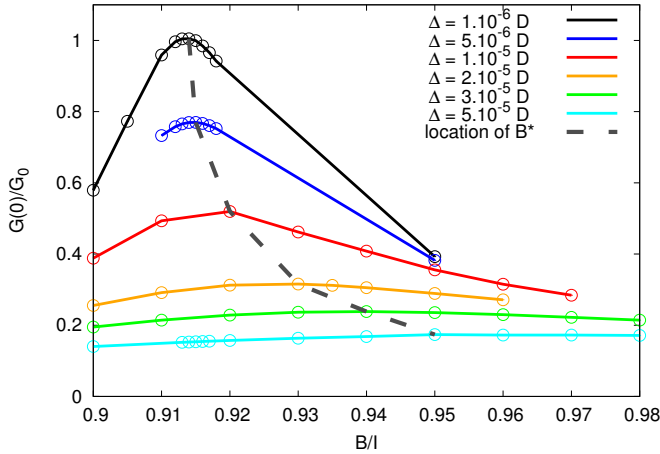


Figure 5: NRG results on the double-dot model with anisotropic exchange: Dependence of the zero-temperature conductance $G(0)$ on external magnetic field B for various Δ ($I = 10^{-3}D$ and $\Gamma = 0.05D$). Lines are only for visual guidance.

Anomalous Temperature Dependence of a Kondo Resonance in a Diradical Molecule

In the following, we present an experimental demonstration of the Kondo effect at a singlet-triplet degeneracy, measured in the diradical single-molecule junction described in the Experimental Methods. We show that the temperature dependence of this Kondo effect strongly deviates from the standard spin-1/2 Kondo effect and we show that this deviation may stem

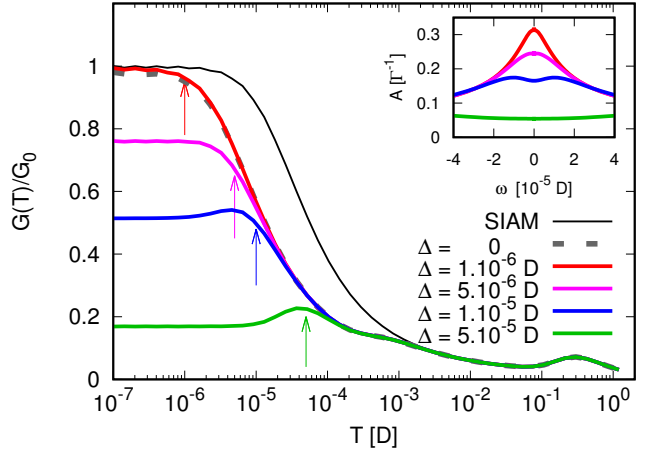


Figure 6: NRG results on the double-dot model with anisotropic exchange: Temperature dependence of the conductance for selected values of Δ ($I = 10^{-3}D$ and $\Gamma = 0.05D$). The magnetic field has been tuned to the corresponding value of resonant $B^*(\Delta)$ from Figure 5. The temperature equivalent to Δ is indicated by arrows. The inset shows the spectral functions at zero-temperature.

from the anisotropic exchange discussed in the previous section.

The diradical molecule used for these measurements consists of two unpaired spins in its ground state. When embedded in a single-molecule junction, the spins in the diradical molecule have a relatively weak exchange coupling $I \sim 1$ meV. As a result, the energies of the spin singlet and one projection of the spin triplet can become degenerate in an achievable magnetic field, as schematically depicted in Scheme 1c. This property opens up the possibility to experimentally observe the singlet-triplet Kondo effect in the diradical molecule.

We probe the spin states of the single-molecule device by measuring the differential conductance (dI/dV) as a function of V and B . The results of this experiment are shown in Figure 7, which contains two dI/dV maps of the same device, recorded at different gate voltages $V_g = -1.7$ V (a) and $V_g = -2.8$ V (b). First, we focus on Figure 7a, which at $B = 0$ T shows a stepwise increase in the dI/dV at $V \approx \pm 0.7$ mV, resulting from added transport channels involving excited states. The ex-

citation steps split as the magnetic field is increased and follow three different slopes. This splitting is a clear manifestation of the Zeeman effect in a spin system with a singlet ground state and a triplet excited state, with an excitation energy equal to the exchange coupling $I \approx 0.7$ meV. At about $B \approx 6.6$ T one projection of the triplet state becomes degenerate in energy with the singlet state and at even higher magnetic fields this projection becomes the new spin ground state. Only two spin excitations are observed after this spin ground-state transition ($B \gtrsim 6.6$ T), as expected from the spin selection rules.³⁷

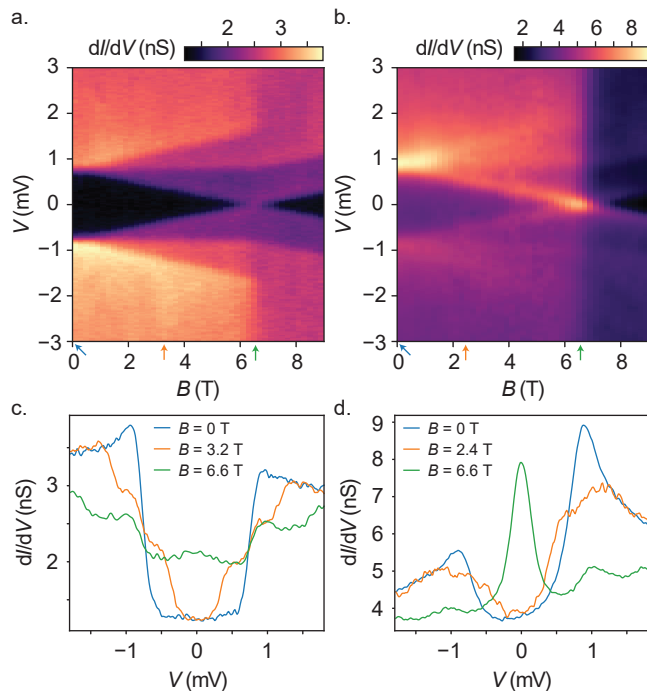


Figure 7: (a,b): Experimental differential conductance (dI/dV) maps showing the magnetic field evolution of the spin excitations between the singlet and triplet states in the diradical single-molecule device, measured at (a) $V_g = -1.7$ V and (b) $V_g = -2.8$ V. In part b, the singlet-triplet Kondo resonance appears at $B \approx 6.6$ T. (c,d) dI/dV spectra at different magnetic fields, corresponding to vertical line-cuts of the dI/dV maps in (a) and (b), respectively. The magnetic fields at which the spectra in (c) and (d) are recorded are indicated by the colored arrows in (a) and (b), respectively.

By changing the gate voltage we were able to tune the single-molecule device closer to a

charge degeneracy point, which typically results in an increase of the overall conductance and a stronger Kondo coupling. This behavior can be observed in the dI/dV map of Figure 7b, which is recorded at $V_g = -2.8$ V. The excitation steps seen in Figure 7a appear in Figure 7b as peaks rather than steps. These peaks are fingerprints of higher-order transport processes, which give rise to Kondo correlations.³⁸ At the singlet-triplet degeneracy ($B \approx 6.6$ T), a zero-bias resonance develops, which can be attributed to the singlet-triplet Kondo correlations.

The low-temperature behavior of the singlet-triplet Kondo effect is equivalent with the low-temperature behavior of a standard spin-half Kondo effect.¹² Our theoretical results on the DQD confirm this equivalence, as long as $T \ll I$ (see Figure 2). Accordingly, the linear conductance as a function of temperature should approximately obey the well-known universal curve³⁹

$$G(T) = G_0 \left[1 + (2^{1/s} - 1) \left(\frac{T}{T_0} \right)^2 \right]^{-s} + G_b, \quad (9)$$

where T_0 is the approximate Kondo temperature, G_b the background conductance, and $s = 0.22$. To experimentally obtain $G(T)$, we recorded dI/dV spectra at fixed $B = 6.6$ T and $V_g = -2.8$ V at various temperatures. The linear conductance was determined by fitting the Kondo peaks to Lorentzian functions and by extracting the peak height to estimate $G(T) - G_b$. The obtained values are normalized to G_0 and plotted in Figure 8a, along with the universal curve with the spin-1/2 value $s = 0.22$ (blue dashed line) and a modified universal curve with $s = 0.7$ (red full line). Remarkably, the experimental data strongly deviates from the universal curve for a standard spin-1/2 system ($s = 0.22$). A good agreement with the experimental data is found by choosing a significantly higher value for the empirical parameter s , which illustrates the anomalous behavior of this Kondo effect.

Here, we propose an explanation for the anomalous temperature dependence, based on comparison with the theoretical results from

previous sections. The main panel in Figure 8b shows how $G(T)$ (thin solid lines) in NRG calculations is influenced by increasing the anisotropic exchange Δ . The low-temperature conductance decreases for higher Δ and a bump appears at $T \sim 10^{-5}D$ for the blue and green curves. We find that in a restricted temperature range, the NRG curves can be well approximated by Eq. (9) with $s > 0.22$. The corresponding fits are drawn in the main panel of Figure 8b as thick solid lines. The small panels of Figure 8b show the normalized NRG results (plus signs) for each Δ , along with the fit (solid line) to Eq. (9) and the corresponding s values. This analysis effectively shows that nonzero values of Δ may result in significantly higher values of s coming from the fits. From this observation we conclude that the presence of an anisotropic exchange interaction is a possible explanation for the anomalous temperature dependence of the singlet-triplet Kondo effect observed in this experiment.

Discussion of the Temperature Dependences

The larger values of s which result from fitting the theoretical temperature dependences [Figure 8b, main panel] can be attributed to two effects: First, the $G(T)$ does not reach the maximum value G_0 due to the anisotropic exchange between the two spins. Second, the high-temperature minimum of $G(T)$ in the restricted temperature range is larger than in the standard case (*i.e.*, SIAM), because of the bump caused by spin excitations. We conclude that the interval of temperatures in which an apparently anomalous behavior can be observed is set by two energy scales: Δ and I . It follows that for the molecular junction studied here, $I \gtrsim 0.4$ meV (corresponding to the highest temperature 4.2 K). This bound is consistent with the value of $I = 0.7$ meV given by the zero-field splitting in Figure 7. Similarly, we can estimate Δ : based on Figure 6 we deduce that Δ marks the onset of the conductance decrease. Consequently, from Figure 8a we get $\Delta \approx 0.4T_0 = 20$ μ eV. This value is more difficult to compare. We remark that spin-orbit

interaction in planar graphene-related systems also lies in the sub-millielectronvolt range.⁴⁰ In principle, lowering the temperature below Δ could lead to splitting of the zero-bias peak as seen in Figure 6, allowing the more precise determination of Δ .

As we argued in the Methods section, the chosen form of the AX in Eq. (4) is not generic and other terms (such as $\hat{S}_1^x \hat{S}_2^y$) can be expected in the molecular junction. Arguments based on molecular symmetry are not applicable here because the molecular geometry is in general distorted due to binding to the leads. Moreover, anisotropic g -tensors could also result from spin-orbit interaction. Naturally, these different anisotropy terms can not be easily disentangled in a transport measurement. However, as long as the anisotropies are weak (compared to I), their main effect is the avoided crossing with the energy scale Δ . On the basis of these considerations we propose that the anomalous temperature dependence observed in the molecular diradical junction is caused by spin anisotropy terms with a characteristic energy scale $\Delta \approx 20$ μ eV (for a given direction of the external magnetic field).

As an alternative scenario of the anomalous temperature dependence of the conductance we mention two-channel Kondo (2CK) physics. As we argued in Methods section, the 2CK effect can be manifested in a smaller portion of the parameter space. Mitchell *et al.*⁵ found a temperature dependence similar to that in Figure 8 at the so-called quantum-interference node. The latter represents a special point of the molecular 2CK, which can be reached by tuning the gate voltage. In our case, the gate voltage was not tuned, and therefore, we think that an intrinsic mechanism, the anisotropic exchange, is more plausible. Moreover, the theoretical results of this work apply to a wider parametric window.

Conclusions

We have analyzed the double quantum dot model at the singlet-triplet crossing in the regime of strong quantum fluctuations (Kondo

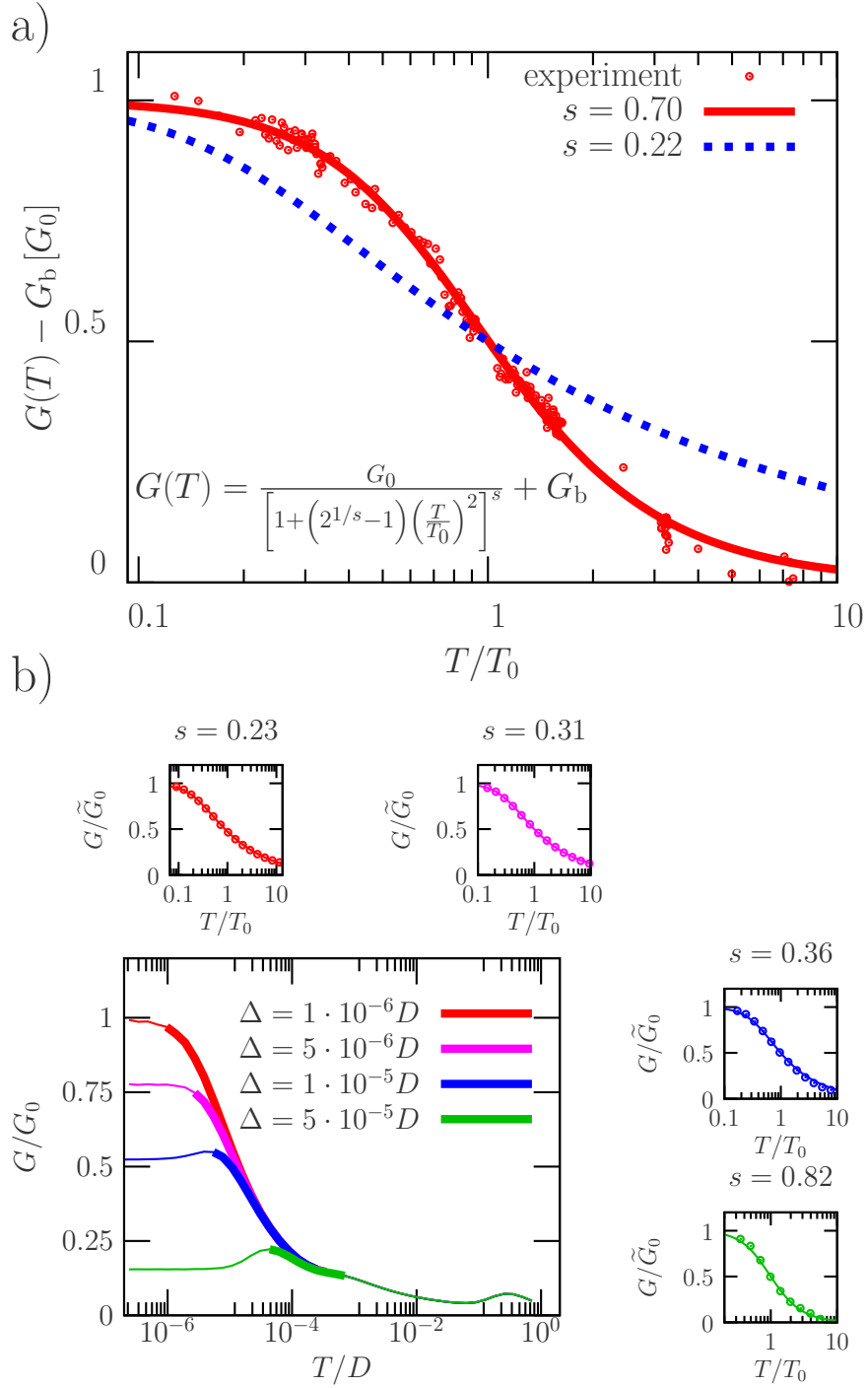


Figure 8: Temperature dependence of singlet-triplet Kondo conductance peaks. (a) Experimental temperature dependence of the conductance of a diradical molecule (red circles) and its fit by the shown empirical equation (red line) with resulting values $s = 0.7$, $T_K = 0.6$ K and $G_0 = 4.9$ nS. The temperature dependence strongly deviates from the universal curve of a spin-1/2 Kondo effect with $s = 0.22$ (dashed blue line). (b) Theoretical temperature dependence of the double quantum dot's conductance. Large plot reproduces Figure 6 showing the effect of anisotropic exchange (thin lines) and the corresponding fits (bold symbols) by Eq. (9) (with the exponent s as a free parameter) for restricted temperature ranges resembling the experiment in panel (a). Small plots show the same temperature dependences of renormalized conductance (\tilde{G}_0 denotes the fitted conductance span in the given interval) for corresponding values of Δ (by color coding) only in the restricted temperature intervals. NRG conductances (points) are fitted (continuous lines) by Eq. (9) with the optimal values of s stated above the plots. Obviously, the increasing values of Δ give by this fitting procedure larger values of s .

effect) with the numerical renormalization group. We have focused on the shift of the singlet-triplet degeneracy, which can be interpreted as an effective magnetic field generated by the leads. Its parametric dependence is non-trivial (apparently non-perturbative), pointing to the role of strong quantum fluctuations. When the external magnetic field is tuned to the degeneracy and Kondo plateaus emerge in the conductance, the two dots still exhibit a sizable spin-polarization. This is surprising, in view of the traditional picture of Kondo-screened moments.

Furthermore, we have studied the effect of an anisotropic exchange (AX). Our data shows that the singlet-triplet Kondo effect is stable against weak AX. The AX of the order of T_K causes lowering of the Kondo plateaus in the temperature dependence of the conductance, $G(T)$. The calculated temperature dependences $G(T)$ bear a strong imprint of the two low-energy scales, Δ and the exchange I .

We have presented experimental data on a molecular junction containing an organic diradical coupled to Au leads. The differential conductance as a function of magnetic field shows a characteristic fingerprint of the singlet-triplet splitting. The zero-bias resonance at the singlet-triplet degeneracy point has a temperature dependence which deviates greatly from the universal curve expected for standard spin-1/2 Kondo systems. We propose an explanation based on the lowering of the conductance plateaus caused by anisotropy terms.

Acknowledgments

We gratefully acknowledge support from the PRIMUS/Sci/09 programme of the Charles University (R.K.) and from the Czech Science Foundation by Grant No. 16-19640S (T.N. and P.Z.). The experimental work (J.dB., R.G., H.S.J.vdZ.) was supported by the Netherlands Organisation for Scientific Research (NWO/OCW), as part of the Frontiers of Nanoscience program, and the ERC Advanced Grant agreement number 240299 (Mols@Mols). We thank J. Veciana and C. Rovira for the synthesis of the diradical molecule and M. Žonda

for his substantial help with setting up the NRG calculations at the beginning of the project.

References

- (1) Roch, N.; Florens, S.; Costi, T. A.; Wernsdorfer, W.; Balestro, F. Observation of the underscreened Kondo effect in a molecular transistor. *Phys. Rev. Lett.* **2009**, *103*, 197202.
- (2) Mugarza, A.; Robles, R.; Krull, C.; Korytár, R.; Lorente, N.; Gambardella, P. Electronic and magnetic properties of molecule-metal interfaces: Transition-metal phthalocyanines adsorbed on Ag(100). *Phys. Rev. B* **2012**, *85*, 155437.
- (3) Minamitani, E.; Tsukahara, N.; Matsunaka, D.; Kim, Y.; Takagi, N.; Kawai, M. Symmetry-driven novel Kondo effect in a molecule. *Phys. Rev. Lett.* **2012**, *109*, 086602.
- (4) Roch, N.; Florens, S.; Bouchiat, V.; Wernsdorfer, W.; Balestro, F. Quantum phase transition in a single-molecule quantum dot. *Nature* **2008**, *453*, 633.
- (5) Mitchell, A. K.; Pedersen, K. G.; Hedegård, P.; Paaske, J. Kondo blockade due to quantum interference in single-molecule junctions. *Nature Communications* **2017**, *8*, 15210.
- (6) Alexander, S.; Anderson, P. Interaction between localized states in metals. *Phys. Rev.* **1964**, *133*, A1594.
- (7) Jayaprakash, C.; Krishna-murthy, H. R.; Wilkins, J. W. Two-Impurity Kondo Problem. *Phys. Rev. Lett.* **1981**, *47*, 737.
- (8) Vojta, M.; Bulla, R.; Hofstetter, W. Quantum phase transitions in models of coupled magnetic impurities. *Phys. Rev. B* **2002**, *65*, 140405.
- (9) Hofstetter, W.; Schoeller, H. Quantum Phase Transition in a Multilevel Dot. *Phys. Rev. Lett.* **2001**, *88*, 016803.

- (10) Varma, C.; Nussinov, Z.; Van Saarloos, W. Singular or non-Fermi liquids. *Physics Reports* **2002**, *361*, 267.
- (11) Langwald, H.-T.; Schnack, J. Magnetization curves of deposited finite spin chains. *arXiv preprint arXiv:1312.0864* **2013**,
- (12) Pustilnik, M.; Avishai, Y.; Kikoin, K. Quantum Dots with Even Number of Electrons: Kondo Effect in a Finite Magnetic Field. *Phys. Rev. Lett.* **2000**, *84*, 1756.
- (13) Pustilnik, M.; Glazman, L. Kondo effect induced by a magnetic field. *Phys. Rev. B* **2001**, *64*, 045328.
- (14) Yarkony, D. R. Diabolical conical intersections. *Rev. Mod. Phys.* **1996**, *68*, 985.
- (15) Armitage, N.; Mele, E.; Vishwanath, A. Weyl and Dirac semimetals in three-dimensional solids. *Rev. Mod. Phys.* **2018**, *90*, 015001.
- (16) Volovik, G. E. *The universe in a helium droplet*, 2nd ed.; Oxford University Press, 2009; Vol. 117 of International Series of Monographs on Physics.
- (17) Yosida, K. *Theory of Magnetism*; Springer series in solid-state sciences; Springer, 1996.
- (18) Herzog, S.; Wegewijs, M. Dzyaloshinskii–Moriya interaction in transport through single-molecule transistors. *Nanotechnology* **2010**, *21*, 274010.
- (19) Scherübl, Z.; Pályi, A.; Frank, G.; Lukács, I.; Fülöp, G.; Fülöp, B.; Nygård, J.; Watanabe, K.; Taniguchi, T.; Zaránd, G. et al. Observation of spin-orbit coupling induced Weyl points and topologically protected Kondo effect in a two-electron double quantum dot. *arXiv:1804.06447* **2018**,
- (20) Stevanato, C.; Leijnse, M.; Flensberg, K.; Paaske, J. Finite-bias conductance anomalies at a singlet-triplet crossing. *Phys. Rev. B* **2012**, *86*, 165427.
- (21) Rajca, A. Organic Diradicals and Polyradicals: From Spin Coupling to Magnetism? *Chemical Reviews* **1994**, *94*, 871–893.
- (22) Gallagher, N. M.; Bauer, J. J.; Pink, M.; Rajca, S.; Rajca, A. High-Spin Organic Diradical with Robust Stability. *Journal of the American Chemical Society* **2016**, *138*, 9377–9380.
- (23) Gaudenzi, R.; de Bruijkere, J.; Reta, D.; Moreira, I. d. P.; Rovira, C.; Veciana, J.; van der Zant, H. S.; Burzurí, E. Redox-Induced Gating of the Exchange Interactions in a Single Organic Diradical. *ACS Nano* **2017**, *11*, 5879.
- (24) Žitko, R. NRG Ljubljana - open source numerical renormalization group code; nr-gljubljana.ijs.si.
- (25) Žitko, R.; Pruschke, T. *Phys. Rev. B* **2009**, *79*, 085106.
- (26) Weichselbaum, A.; von Delft, J. Sum-Rule Conserving Spectral Functions from the Numerical Renormalization Group. *Phys. Rev. Lett.* **2007**, *99*, 076402.
- (27) Veciana, J.; Rovira, C.; Ventosa, N.; Crespo, M. I.; Palacio, F. Stable polyradicals with high-spin ground states. 2. Synthesis and characterization of a complete series of polyradicals derived from 2, 4, 6-trichloro- $\alpha, \alpha', \alpha', \alpha'', \alpha''$ -hexakis (pentachlorophenyl) mesitylene with S= 1/2, 1, and 3/2 ground states. *Journal of the American Chemical Society* **1993**, *115*, 57.
- (28) Park, H.; Lim, A. K. L.; Alivisatos, A. P.; Park, J.; McEuen, P. L. Fabrication of metallic electrodes with nanometer separation by electromigration. *Applied Physics Letters* **1999**, *75*, 301.
- (29) O’Neill, K.; Osorio, E. A.; van der Zant, H. S. J. Self-breaking in planar few-atom Au constrictions for nanometer-spaced electrodes. *Applied Physics Letters* **2007**, *90*, 133109.

- (30) Korytár, R.; Lorente, N.; Gauyacq, J.-P. Many-body effects in magnetic inelastic electron tunneling spectroscopy. *Phys. Rev. B* **2012**, *85*, 125434.
- (31) Chung, C.-H.; Hofstetter, W. Kondo effect in coupled quantum dots with RKKY interaction: Effects of finite temperature and magnetic field. *Phys. Rev. B* **2007**, *76*, 045329.
- (32) Golovach, V. N.; Loss, D. Kondo effect and singlet-triplet splitting in coupled quantum dots in a magnetic field. *EPL (Europhysics Letters)* **2003**, *62*, 83.
- (33) In Ref.⁴¹ the effective field was analyzed in a hard-axis single spin impurity.
- (34) Costi, T. Kondo effect in a magnetic field and the magnetoresistivity of Kondo alloys. *Phys. Rev. Lett.* **2000**, *85*, 1504.
- (35) Costi, T. A. Magnetotransport through a strongly interacting quantum dot. *Phys. Rev. B* **2001**, *64*, 241310.
- (36) Moore, J. E.; Wen, X.-G. Anomalous Magnetic Splitting of the Kondo Resonance. *Phys. Rev. Lett.* **2000**, *85*, 1722.
- (37) Gaudenzi, R.; Misiorny, M.; Burzurí, E.; Wegewijs, M. R.; van der Zant, H. S. Transport mirages in single-molecule devices. *The Journal of Chemical Physics* **2017**, *146*, 092330.
- (38) Ternes, M. Spin excitations and correlations in scanning tunneling spectroscopy. *New Journal of Physics* **2015**, *17*, 063016.
- (39) Goldhaber-Gordon, D.; Göres, J.; Kastner, M.; Shtrikman, H.; Mahalu, D.; Meirav, U. From the Kondo regime to the mixed-valence regime in a single-electron transistor. *Phys. Rev. Lett.* **1998**, *81*, 5225.
- (40) Castro Neto, A. H.; Guinea, F.; Peres, N. M. R.; Novoselov, K. S.; Geim, A. K. The electronic properties of graphene. *Rev. Mod. Phys.* **2009**, *81*, 109.
- (41) Höck, M.; Schnack, J. Numerical renormalization group calculations of the magnetization of Kondo impurities with and without uniaxial anisotropy. *Phys. Rev. B* **2013**, *87*, 184408.